Available online at www.sciencedirect.com

jmr&t Journal of Materials Research and Technology

www.jmrt.com.br

Original Article

# Determination of fluoride component in the multifunctional refining flux used for recycling aluminum scrap

*Bingbing Wan*[a,b,c,*], *Wenfang Li*[a], *Fangfang Liu*[c,d], *Tiwen Lu*[c,e], *Shuoxun Jin*[a,c], *Kang Wang*[a], *Aihua Yi*[a], *Jun Tian*[a], *Weiping Chen*[c,*]

[a] *School of Materials Science and Engineering, Dongguan University of Technology, Dongguan 523000, China*
[b] *School of Materials Science and Engineering, Xi'an Jiaotong University, Xi'an, 710049, China*
[c] *Guangdong Key Laboratory for Advanced Metallic Materials Processing, South China University of Technology, Guangzhou 510640, China*
[d] *Department of Electromechanical Engineering, Guangdong University of Science and Technology, Dongguan 523083, China*
[e] *IFW Dresden, Institute for Complex Materials, Helmholtzstraße 20, D-01069, Dresden, Germany*

ARTICLE INFO

*Article history:*
Received 4 November 2019
Accepted 23 January 2020
Available online 7 February 2020

*Keywords:*
Aluminum recycling
Multifunctional refining flux
Fluoride salt
Interfacial tension
Coalescence behavior

ABSTRACT

In this paper, the optimum fluoride component in the multifunctional refining flux used for recycling aluminum scrap was determined. Theoretical analysis of solid fluxing shows that strong stripping ability of oxide layer on aluminum surface for the flux and appropriate interfacial tensions between Al melt / inclusion ($\sigma_{M\text{-}I}$), flux / inclusion ($\sigma_{F\text{-}I}$), and flux / Al melt ($\sigma_{F\text{-}M}$) are indispensable for making the flux achieve the properties of covering, drossing, and cleaning simultaneously. In term of four preliminarily selected fluoride salts, i.e., KF, $AlF_3$, $K_3AlF_6$ and $KAlF_4$, the results of interfacial tension measurements indicates that, combined addition of A-type fluoride (KF) and B-type fluoride ($AlF_3$, $K_3AlF_6$ and $KAlF_4$) to equimolar NaCl-KCl can just offset the shortage of single addition of KF which means worsening the separating effect of flux from melt surface and weakening the wettability of flux on the inclusions due to the lower $\sigma_{F\text{-}M}$ and the higher $\sigma_{F\text{-}I}$ respectively. Additionally, coalescence behaviors of aluminum droplets in molten fluxes reveals that, KF, $K_3AlF_6$ or $KAlF_4$ possesses stronger stripping ability of oxide layer, while the stripping ability of oxide layer for $AlF_3$ is weaker. Ultimately, the combination of KF with $K_3AlF_6$ or/and $KAlF_4$ is ascertained to be an optimum selection for fluoride component in the multifunctional refining flux.



* *Corresponding author.*
E-mails: 18665566386@163.com, 2018309@dgut.edu.cn (B. Wan), mewpchen@scut.edu.cn (W. Chen).
https://doi.org/10.1016/j.jmrt.2020.01.082

## 1. Introduction

Aluminum is one of the most significant non-ferrous metals and it is currently being extensively used in the automotive, aerospace, packaging, electronics and construction industries [1–4]. The recycling of aluminum scraps has attracted more and more attention of researchers and governments in the word for reduced emissions and waste disposal, resource regenerating and energy savings [5]. Nevertheless, during the production of recycled aluminum, as for aluminum scraps covered with moisture and oil stain, aluminum melt can easily react with gaseous $H_2O$ and oxygen to form oxide inclusions [6], and oxide films on melt surface can be entrained in the bulk liquid due to surface turbulence [4,7–9]. In addition, nitrides, carbides, chlorides, fluorides and borides also exist in the melt [10]. Consequently, considerable amounts of solid inclusions (mainly $Al_2O_3$), as dispersed particles or oxide films, are usually suspended in the melt, which will cause a variety of problems, including loss of fluidity and feeding properties, increase in porosity, leakage defects, poor machinability, and reduction in the mechanical properties [7,11–13]. Therefore, the removal of solid inclusions from the aluminum melt is of vital importance to ensure metallurgical quality of recycled aluminum.

To date, the most popular process of removing solid inclusions from aluminum melt is solid flux refining [14]. In general, there exist three major categories of solid fluxes such as covering fluxes, drossing fluxes and refining fluxes depending on their compositions and functions [15,16]. In terms of conventional process of melt purification, these three salt fluxes are employed coordinately to obtain better metal cleanliness. Firstly, covering fluxes are used to form a molten layer to prevent melt oxidation and hydrogen pick-up, and then refining fluxes are delivered into the melt to eliminate non-metallic inclusions. Finally, drossing fluxes are spread evenly onto the dross layer of the melt surface to reduce the aluminum content of dross and facilitate removal of dross. Apparently, the adoption of monofunctional solid fluxes will complicate the melt purification, thus resulting in longer melt treatment time, higher melt handing costs and greater labor intensity. Furthermore, excessive usage of solid fluxes can probably lead to flux inclusion and serious burning loss of aluminum. To overcome these drawbacks, the multifunctional refining flux which possesses the properties of covering, drossing, and cleaning simultaneously is urgent to be investigated.

Solid fluxes for aluminum alloys are primarily blends of chlorides and fluorides with additives to instill specific properties [15–18]. Numerous studies have confirmed that fluoride components play a crucial role in the fluxes. In the studies of Li et al. [14] and Utigard et al. [15], after NaF, $Na_3AlF_6$, $CaF_2$ or $Na_2SiF_6$ addition to the chloride flux, the inclusion removal property of the molten flux was improved due to the decreasing of the wetting angle between molten salt and solid inclusion and the work of adhesion of the Al melt-inclusion interface. Tenorio et al. [19] found that fluoride additions to molten flux could improve the dissolution rate and corrosive attack of alumina. This conclusion is in accordance with the previous report by Ye and Sahai [20]. Roy and Sahai [21], Besson et al. [22] and Xiao et al. [23,24] observed that NaF, KF, $MgF_2$ or $Na_3AlF_6$ additions to equimolar NaCl-KCl could enhance the coalescence of metal droplets in molten salts and cause the formation of dry dross [11]. Additionally, Utigard et al. [15] and Tenorio et al. [19] pointed out that, as for equimolar mixtures of NaCl-KCl, the addition of NaF and KF (up to 5 wt.%) significantly decreased the viscosity of the molten flux while $CaF_2$ or $Na_2SiF_6$ addition increased the viscosity of the molten flux, which could affect coalescence behaviors of metal droplets in salts and subsequent salt/metal separation. However, to our knowledge, currently there is still a lack of thorough systematic investigations on how fluoride components in the flux influence the behaviors of covering, drossing, and cleaning simultaneously. In addition, some alkali and alkaline earth elements, i.e. Li, Na, Ca and Mg, are common dissolved unwanted impurities in aluminum melt, which can bring about the deterioration of casting and processing properties of aluminum [25–27]. Nowadays, commercially available refining fluxes usually contain fluoride components such as LiF, NaF, $Na_3AlF_6$, $CaF_2$, $MgF_2$, $Na_2SiF_6$ and $K_2SiF_6$. Accordingly, common impurity elements may be introduced into the melt, and toxic $SiF_4$ can be released into the air.

In view of the above discussion, it can be observed that, the development and application of the multifunctional refining flux hasn't yet been received considerable attentions, and hence the fundamental information related to the influence of fluoride component on the flux's multifunctional performances is virtually non-existent, resulting in inadequate support for the selection of fluoride component. Thus, the present study firstly sought the necessary prerequisites for making the recycled aluminum refining flux achieve multifunctional performances by means of systematic theoretical analysis on fluxing treatment. On this basis, the optimum fluoride component free from unwanted elements such as Li, Na, Ca, Mg and Si in the multifunctional flux was determined according to the discussion on the results of interfacial tension measurements and coalescence tests.

## 2. Experimental

### 2.1. *Differential scanning calorimetry (DSC) analysis*

In order to obtain the melting characteristic of the salt flux, measurement by differential scanning calorimetry (NETZSCH STA449C) was performed on about 10 mg salts in a temperature range from 25 °C to 800 °C with a heating rate of 10 °C/min under an argon atmosphere. By analyzing the DSC heating curve, the melting characteristic of the salt flux can be revealed.

### 2.2. *Interfacial tension measurements*

As illustrated in the Fig. 1, the sessile drop method was utilized to measure the interfacial tension between molten flux and Al melt ($\sigma_{F\text{-}M}$). Based on the Laplace's formula, Bashforth and Adams [28] have proposed the Bashforth-Adams equation concerning the shape of droplet under the action of gravity, and this equation can be expressed as:

$$\frac{b}{R_1} + \frac{\sin\varphi}{X/b} = 2 + \frac{\Delta\rho g b^2}{\sigma_{F-M}}\left(\frac{Z}{b}\right) \quad (1)$$

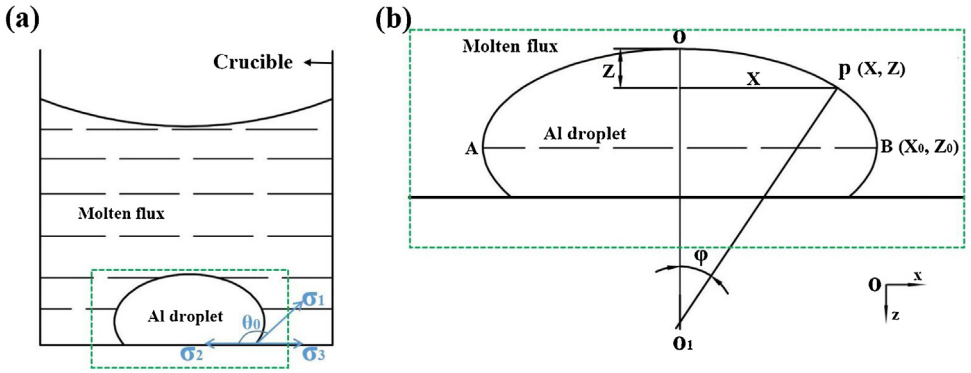


**Fig. 1 – (a) Schematic of the experimental set-up for interfacial tension measurement; (b) Enlarged view of the green square in (a).**

Let $\frac{\Delta\rho g b^2}{\sigma_{F-M}}$ be called $\beta$, which is a shape factor. Hence:

$$\sigma_{F-M} = \frac{\Delta\rho g b^2}{\beta} \quad (2)$$

In the Eq. (1), X and Z are the horizontal and vertical coordinate of any point P in a meridional section of the surface of the droplet respectively, $R_1$ is the radius of curvature of the meridional section at the point P, and $\varphi$ is the included angle between the normal through the point P ($PO_1$) and the symmetry axis ($OO_1$); $b$ is the radius of curvature at the origin of the droplet (Point O); $\Delta\rho$ is the density difference between molten salt and Al melt; $g$ is the gravitational acceleration. Special B-A table has already been made [28], which depicts the values of $X/b$, $Z/b$ and $X/Z$ corresponding to different values of $\beta$ and $\varphi$. The getting of the $\sigma_{F\text{-}M}$ value mainly consists of two procedures: (I) Depending on the B-A table, inspecting the $\beta$ value corresponding to the X/Z value under the condition of $\varphi = 90°$, and then inspecting the values of $X/b$ and $Z/b$ corresponding to the known $\beta$ value and $\varphi = 90°$, thus obtaining the value of $b$; (II) Calculating the value of $\sigma_{F\text{-}M}$ by the Eq. (2).

In our experiments, firstly approximately 100 g of dried solid flux together with a solid piece (10–15 g) of pure aluminum was adequately melted using an alumina cylindrical crucible (Ø61 mm × 61 mm) in a resistance furnace under an argon environment at 740 °. After a 30 min holding time, the crucible was carefully taken out of the furnace and air cooled to room temperature. Then the crucible content was crushed, rinsed and dried, thus obtaining an ellipsoidal aluminum bead. Subsequently, the pictures of the aluminum bead were taken, and the profile of aluminum bead was generally deemed to be nearly identical to that of corresponding aluminum droplet in molten flux herein [29]. On the basis of the obtained geometrical dimensions of the bead, as $X_0$ and $Z_0$ corresponding to $\varphi = 90°$ noted in Fig. 1(b), the values of $\beta$ and $b$ can be gained by the B—A table. Besides, the density of pure aluminum melt at 740 °C was 2.36 g/cm$^{-3}$ [30], and the density of molten flux was measured by an RTW-10 type synthetic test instrument for melt physical property relying on the Archimedes method. Ultimately, according to the known values of $\Delta\rho$, $\beta$, $b$ and $g$, the $\sigma_{F\text{-}M}$ value was calculated by the Eq. (2). For each salt flux, three group of $X_0$ and $Z_0$ through three repetitive tests were measured to minimize the errors and obtain the average value of $\sigma_{F\text{-}M}$.

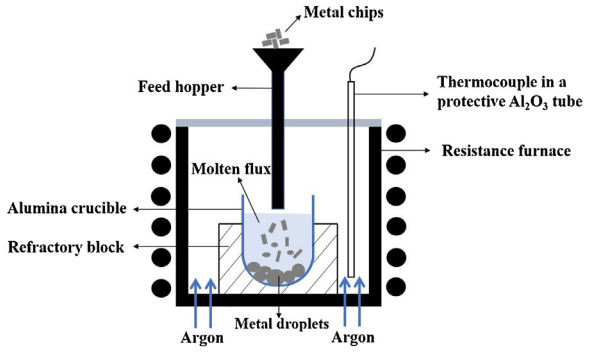


**Fig. 2 – Schematic of the experimental set-up for the coalescence tests.**

In Fig. 1(a), as for the Al droplet in molten flux contained in the alumina crucible, the Young's equation can be written as follows [31]:

$$\sigma_3 = \sigma_2 + \sigma_1 \cos\theta_0 \quad (3)$$

Where $\sigma_1$ ($\sigma_{F\text{-}M}$), $\sigma_2$ and $\sigma_3$ are the interfacial tensions between flux / Al melt, Al melt / inclusion and flux / inclusion respectively, and $\theta_0$ is the wetting angle between Al melt and alumina which can be measured directly from the profile of aluminum bead.

### 2.3. *Measurements of coalescence ability of solid fluxes*

It is generally accepted that coalescence of metal droplets in molten flux is primarily hindered by the oxide layer on metal surface. In order to examine the coalescence ability of different fluxes, aluminum chips with highly oxidized surfaces (due to larger specific surface area) were used as experiment charge. Fig. 2 illustrates the test for coalescence of metal droplets in molten flux. Firstly, 150 g of dried solid flux was adequately melted using an alumina crucible with round bottom in a resistance furnace under argon atmosphere at 800 °. Then 15 g of aluminum chips were introduced into the crucible by a stainless-steel hopper. After a set time, the crucible was

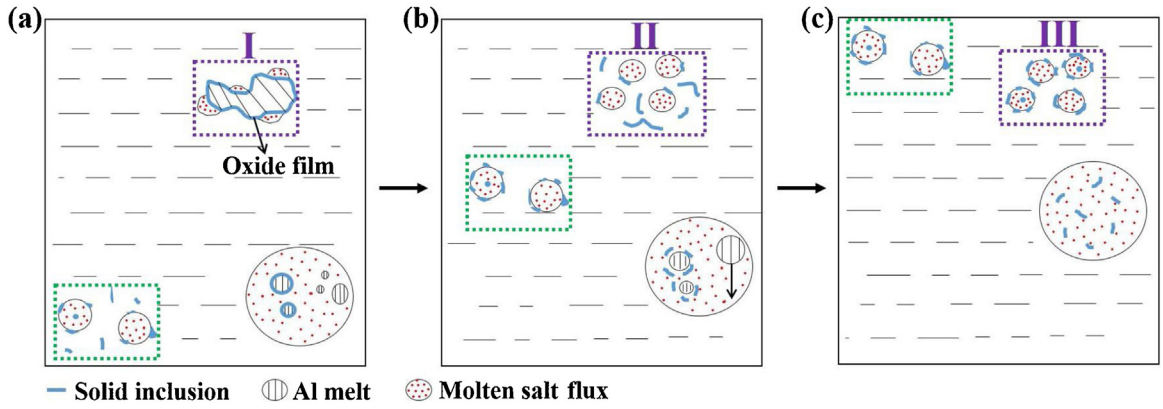


**Fig. 3 – Schematic of inclusion removal by molten salt flux.**

carefully taken out of the furnace and air cooled to room temperature. Subsequently, the crucible content was washed with hot water, and then the metal beads and the oxide residues were filtered and dried. Finally, taking a picture of all the recovered metal beads so as to observe the coalescence effect of aluminum droplets in molten flux which can reflect the coalescence ability of the flux.

## 3. Results and discussion

### 3.1. *Theoretical analysis of solid fluxing*

As we know, inclusion removal from aluminum melt is primarily achieved through physical separation of salt fluxes, which means that inclusions are wetted by molten salts and subsequently floated towards melt surface along with the slag. The process of inclusion removal by molten salt flux is illustrated schematically in Fig. 3. In terms of particulate inclusions and discrete oxide films suspended in the melt, they can be removed directly by the wetting action of fluxes, as marked in green squares. However, for the scrap aluminum of an intact oxide film, the removal of oxide film, which helps to release the molten aluminum enveloped, should undergo three stages marked in blue squares. At stage I, molten salts are adsorbed onto oxide film. At stage II, continuous oxide film is destroyed and stripped by fluxes. At stage III, discrete oxide films are wetted by molten salts. In addition, note that aluminum droplets are usually trapped within molten salts. Once the oxide layer on aluminum droplet is stripped by molten salts, aluminum droplets will be coalesced into larger droplet, which allows for a faster setting and therefore promotes the salt/metal separation. From the above description, it clearly indicates that, the stripping of oxide layer on aluminum surface and the wetting of solid inclusions are closely related to the inclusion removal process of the flux. Besides, the efficiency of oxide layer removal by the flux can also influence the aluminum content of dross.

#### 3.1.1. *Analysis of spreading, separating, and wetting abilities of the flux*

3.1.1.1. *Spreading property of the flux.* Fig. 4 shows the schematic of the spreading of molten flux on the surface of Al melt. In Fig. 4, $\sigma_{F\text{-}M}$ is the interfacial tension between flux and Al melt, $\sigma_F$ is the surface tension of the flux, $\sigma_M$ is the surface tension of the Al melt, and $\theta$ is the wetting angle between flux and Al melt. According to Young's equation [31], $\cos\theta$ can be determined as:

$$\cos\theta = \frac{\sigma_M - \sigma_{F-M}}{\sigma_F} \tag{4}$$

Based on the Eq. (4), it can be seen that the lower values of $\sigma_{F\text{-}M}$ and $\sigma_F$ and the higher value of $\sigma_M$ can lower the wetting angle ($\theta$), thus improving the spreading property of the flux.

3.1.1.2. *Separating property of the flux.* Fig. 5 shows the schematic of the separation of molten flux from the Al melt surface. Obviously, the spreading and separating behavior of the flux can be regarded as two opposite processes. Therefore, from the Eq. (4), it can be inferred that the higher values of $\sigma_{F\text{-}M}$ and $\sigma_F$ and the lower value of $\sigma_M$ can increase the wet-

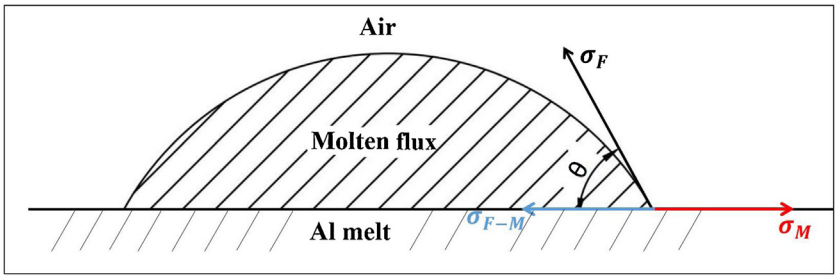


**Fig. 4 – Schematic of the spreading of molten flux on the surface of Al melt.**

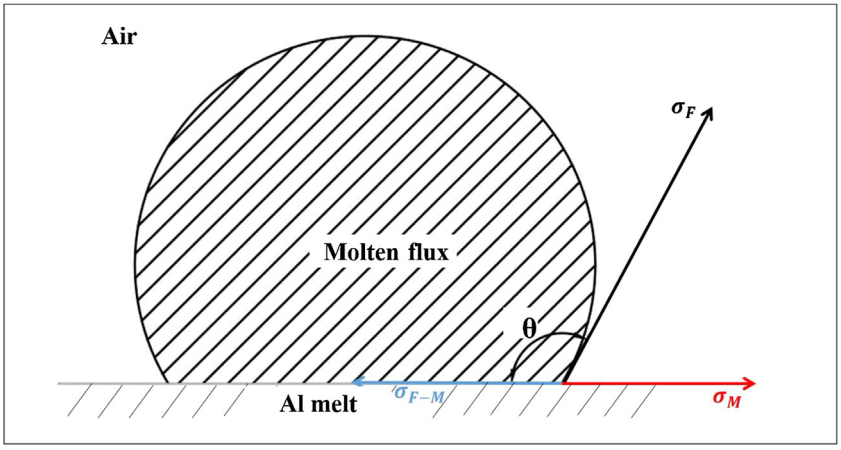


**Fig. 5 – Schematic of the separation of molten flux from the Al melt surface.**

ting angle ($\theta$), thus promoting the separation of the flux from the melt surface.

3.1.1.3. *Wetting property of the flux*. Two types of wetting phenomena, i.e. adhesional or immersional wetting, may occur when the molten fluxes touch solid inclusions in aluminum melt [31]. Fig. 6 shows wetting situation of molten flux on solid inclusion in Al melt. Clearly, the size relationship between the radius of molten salt droplet ($R$) and the length of solid inclusion ($L$) determines the type of wetting [14]. The $R$ can be given by the following expression [32]:

$$R = \sqrt[3]{\frac{3V\sin^3\theta}{\pi(2-3\cos\theta+\cos^3\theta)}} \quad (5)$$

Where $V$ is the volume of molten salt droplet, and $\theta$ is the wetting angle between molten salt and solid inclusion. If $2R < L$, the solid inclusion will be brought into contact with the molten flux. If $2R > L$, the solid inclusion will be completely immersed in the molten flux.

Nevertheless, for both adhesional wetting and immersional wetting, it is universally acknowledged that inclusion removal property of the flux mainly depends on the wetting degree of liquid to solid surface. The better wettability between molten salt and solid inclusion can increase the inclusion removal efficiency, and consequently the wetting angle of flux on inclusion is an important parameter to valuate wetting property. As represented in Fig. 6, $\sigma_{F\text{-}M}$ is the interfacial tension between flux and Al melt, $\sigma_{F\text{-}I}$ is the interfacial tension between flux and inclusion, and $\sigma_{M\text{-}I}$ is the interfacial tension between Al melt and inclusion. According to Young's equation [31], $\cos\theta$ can be determined as:

$$\cos\theta = \frac{\sigma_{M-I}-\sigma_{F-I}}{\sigma_{F-M}} \quad (6)$$

Based on the Eq. (6), it can be seen that the lower values of $\sigma_{F\text{-}M}$ and $\sigma_{F\text{-}I}$ and the higher value of $\sigma_{M\text{-}I}$ can lower the wetting angle ($\theta$), thus improving wetting property of the molten flux on solid inclusion.

**Table 1 – Requirements of interfacial tensions to make the flux achieve superior properties in the Al melt-inclusion-flux system.**

| Properties of the flux | Interfacial tensions | | |
|---|---|---|---|
| | $\sigma_{F\text{-}M}$ | $\sigma_{F\text{-}I}$ | $\sigma_{M\text{-}I}$ |
| Spreading property | Lower value | — | — |
| Separating property | Higher value | — | — |
| Wetting property | Lower value | Lower value | Higher value |

3.1.1.4. *Requirements of interfacial tensions in the Al melt, inclusion, and flux system*. In view of the comprehensive analysis of spreading, separating, and wetting abilities of the flux based on the wetting theory, it is deduced that the interfacial tensions between Al melt / inclusion ($\sigma_{M\text{-}I}$), flux / inclusion ($\sigma_{F\text{-}I}$), and flux / Al melt ($\sigma_{F\text{-}M}$) play a vital role in the aluminum refining process. The requirements of interfacial tensions to make the flux achieve superior properties in the Al melt-inclusion-flux system are listed in Table 1. It can be seen that, the lower value of $\sigma_{F\text{-}M}$ is helpful for flux to spread over the melt surface and remove solid inclusions, while excessive low value of $\sigma_{F\text{-}M}$ makes it difficult for flux to be separated from Al melt. Moreover, the lower value of $\sigma_{F\text{-}I}$ and the higher value of $\sigma_{M\text{-}I}$ are also beneficial for flux to remove solid inclusions.

3.1.2. *Analysis of oxide layer stripping ability of the flux*

From the process of inclusion removal by salt fluxes in Fig. 3, it is clear that oxide layer stripping ability of the flux can exert a significant impact on the inclusion removal and salt/metal separation efficiency. It has been confirmed that aluminum droplets coalescence in molten salts is mainly hindered by thin oxide layers on the droplets [21,22,33,34]. When oxide layers are stripped off, the coalescence can proceed automatically as a consequence of the decreasing of free energy resulting from reduction in surface area. In order to evaluate oxide layer stripping ability of the flux, tests for coalescence of aluminum droplets in molten flux can be implemented. When the alu-

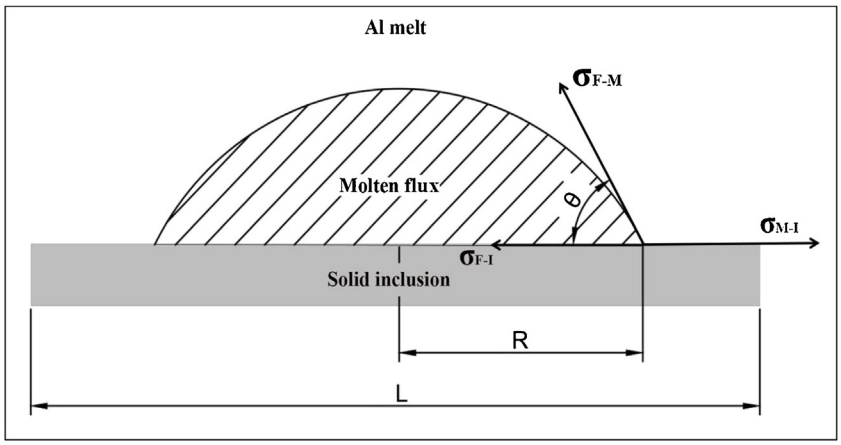


**Fig. 6 – Wetting situation of molten flux on solid inclusion in Al melt.**

minum droplets are settling down in the viscous molten flux, the settling velocity (V) can be formulated as follows [35]:

$$V = \frac{2r^2(\rho_M - \rho_F)g}{9\eta_F} \quad (7)$$

Where $r$ is the droplet radius, $\rho_M$ is the density of aluminum melt, $\rho_F$ is the density of molten flux, $\eta_F$ is the viscosity of molten flux, and $g$ is the gravitational acceleration. Based on the Eq. (7), it can be seen that the lower density and viscosity of molten flux will fasten settlement, thereby favoring the movement of aluminum droplets in molten flux and creating a better coalescence condition [19]. Therefore, for the sake of effectively evaluating oxide layer stripping ability of the flux, the interference of two factors (i.e. density and viscosity of molten flux) to the coalescence of aluminum droplets should be eliminated.

### 3.2. *Determination of fluoride component in the multifunctional refining flux*

From the above theoretical analysis of solid fluxing, it can be seen that, if the salt flux wants to possess the functions of covering, drossing, and cleaning simultaneously, two conditions are indispensable in the Al melt-inclusion-flux system, i.e. appropriate interfacial intensions between Al melt / inclusion, flux / inclusion, and flux / Al melt and strong stripping ability of oxide layers for the flux. Therefore, the multifunctional flux should be of specific ingredients to instill triple properties.

Nowadays, these exist aluminum refining fluxes based on $MgCl_2$-KCl or NaCl-KCl. However, $MgCl_2$ is fairly expensive, so the cost of corresponding refining flux will increase a lot, besides, the hygroscopicity of $MgCl_2$ is higher, resulting in the lumping of the fluxes readily. Therefore, equimolar NaCl-KCl mixture were selected as basic components in our research. Fig. 7(a) presents the DSC heating curve for equimolar NaCl-KCl salts. It reveals the presence of a low-temperature (655 °C) eutectic, which is further confirmed based on the NaCl-KCl binary phase diagram (see Fig. 7(b)), and therefore the flux of lower melting point can be generated. Moreover, chlorides are usually used to improve the fluidity of the flux owing to chlorides' fluidizing effects. Table 2 displays equilibrium constants for the reactions between aluminum and halides at 740 °C which are calculated using HSC Chemistry 6.0 software. As for basic components, it is clearly seen from Table 2 that NaCl and KCl can hardly react with Al melt at 740 °C due to extremely small equilibrium constants for the corresponding reaction (a) and (b). As a result, almost no impurity element (Na) will be introduced into the molten bath.

**Table 2 – Equilibrium constants for the reactions between aluminum and halides at 740 °C.**

| No. | Reactions | Equilibrium constants ($K_{eq}$) |
|---|---|---|
| (a) | $Al(l) + 3NaCl(l) = AlCl_3(l) + 3Na(l)$ | $K_{eq} = 7.16 \times 10^{-24}$ |
| (b) | $Al(l) + 3KCl(l) = AlCl_3(l) + 3K(l)$ | $K_{eq} = 2.14 \times 10^{-27}$ |
| (c) | $Al(l) + 3KF(l) = AlF_3(l) + 3K(l)$ | $K_{eq} = 2.21 \times 10^{-8}$ |
| (d) | $Al(l) + 3NaF(l) = AlF_3(l) + 3Na(l)$ | $K_{eq} = 5.86 \times 10^{-9}$ |

Fig. 8 depicts the coalescence of aluminum chips in equimolar NaCl-KCl salt solution as a function of time. From Fig. 8(a), initial morphology of aluminum chips was described. In Fig. 8(b) and (c), after the chips were immersed in molten salt for 10 and 90 min, the recovered samples exhibited similar morphology with the ones in Fig. 8(a). In contrast to the Fig. 8(b), the chips in Fig. 8(c) got smaller, and a few small metal beads were formed. When chips were immersed in molten salts containing chlorides for a relatively longer time, microcracks formed in the oxide layer because of continuous chemical attack and thermal stresses [21,36]. However, since the strength of oxide layer was high enough, the oxide layer was kept better integrity and not stripped to a significant extent, leading to the outflow of only a small amount of molten aluminum from the cracks in the oxide layer. Therefore, according to the poor coalescence of aluminum droplets in chlorides, it can be concluded that the salts containing only NaCl and KCl barely possess the capability of stripping oxide layer.

In addition to chlorides, fluorides are common and essential additives in refining flux, whose main functions are to improve flux's stripping ability of oxide layer and adjust interfacial tensions between Al melt / inclusion, flux / inclusion, and flux / Al melt. Utigard et al. [15] discovered that, compared with chloride salts, fluoride salts are more reactive in

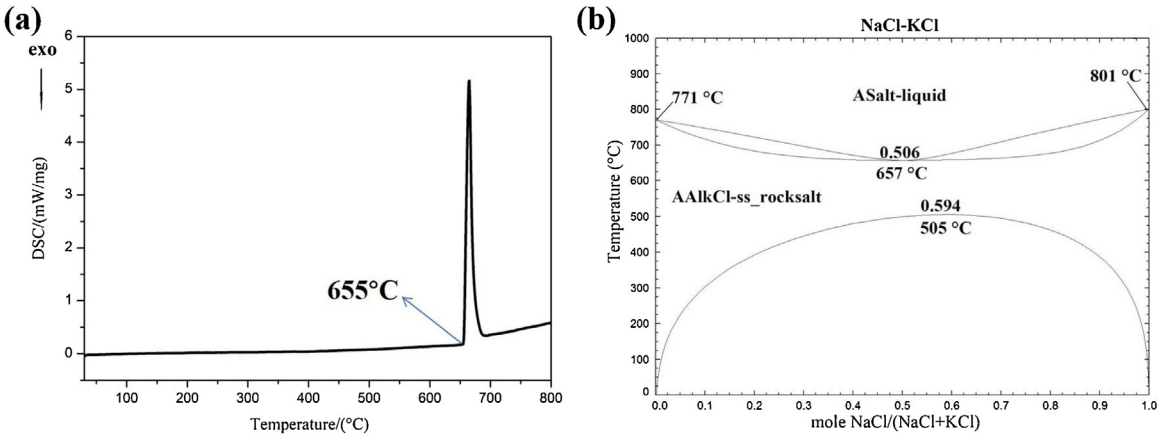


**Fig. 7 – (a) The DSC heating curve for equimolar NaCl-KCl salts; (b) Binary phase diagram of NaCl-KCl.**

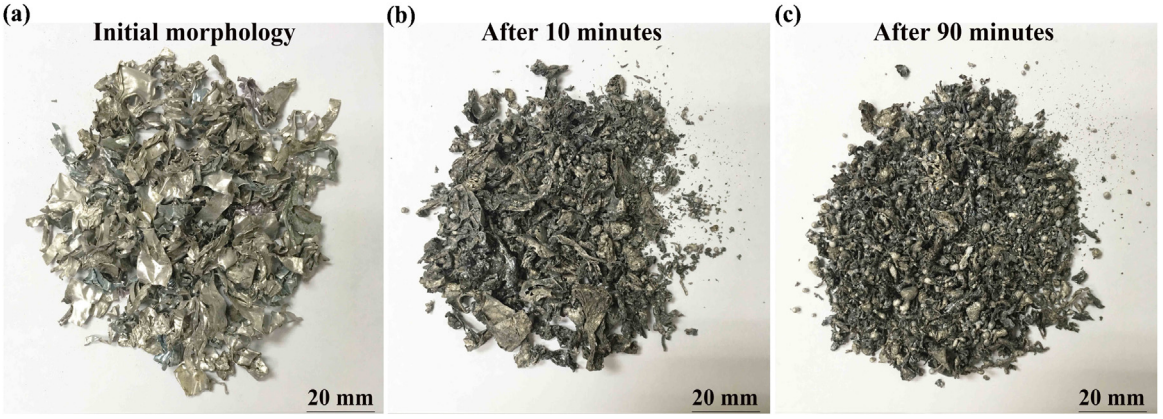


**Fig. 8 – Initial aluminum chips (a) and their coalescence behavior in equimolar NaCl-KCl salt solution (b–c).**

aluminum melt, thus directly introducing alkali and alkaline earth elements such as Li, Na, Ca and Mg in various degree. Owing to adverse impacts of aforementioned impurity elements on the properties of aluminum alloys, fluoride salts free from Li, Na, Ca and Mg are preliminarily selected in our study. Besides, common $K_2SiF_6$ will decompose under high temperature (740 °C), releasing toxic $SiF_4$. Therefore, KF, $AlF_3$, $K_3AlF_6$ and $KAlF_4$ will be discussed detailedly in the following sections.

### 3.2.1. *Test results and discussion of interfacial tensions between flux / Al melt ($\sigma_{F\text{-}M}$) and flux / inclusion ($\sigma_{F\text{-}I}$)*

It has been reported by Roy and Sahai [29] that the interfacial tension between pure Al melt and Alumina ($\sigma_{M\text{-}I}$) at 740 °C is a constant (1659 mN/m). In the Al melt-inclusion-flux system, in order to facilitate the testing and discussion of interfacial tensions, pure aluminum was used as experimental material, and alumina was almost seen as solid inclusions in Al melt. The interfacial tensions between pure Al melt and equimolar NaCl-KCl with addition of KF, $AlF_3$, $K_3AlF_6$ or $KAlF_4$ ($\sigma_{F\text{-}M}$) were measured by the sessile drop method. Subsequently, according to wetting angle between alumina and pure Al melt ($\theta_0$ in Fig. 1(a)), interfacial tension between pure Al melt / Alumina ($\sigma_{M\text{-}I}$), and interfacial tension between flux / pure Al melt

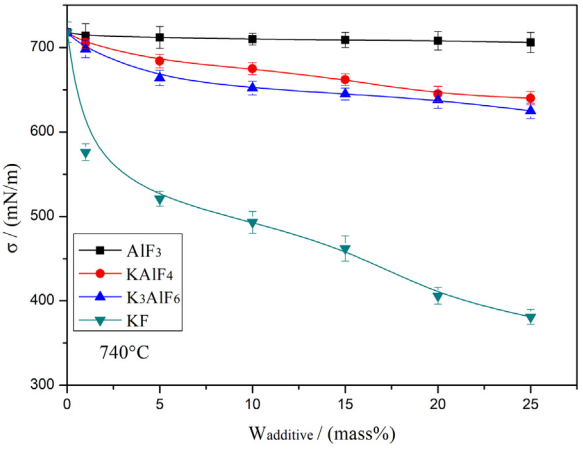


**Fig. 9 – Variation of interfacial tension between flux and pure Al melt at 740 °C as a function of additives in equimolar NaCl-KCl salt solution.**

($\sigma_{F\text{-}M}$), interfacial tension between flux / alumina ($\sigma_{F\text{-}I}$) at 740 °C was calculated by Young's equation (see Eq. (3)).

Fig. 9 shows the variation of interfacial tension between flux and pure Al melt ($\sigma_{F\text{-}M}$) at 740 °C as a function of mass% fluoride addition to equimolar NaCl-KCl. Interfacial tension

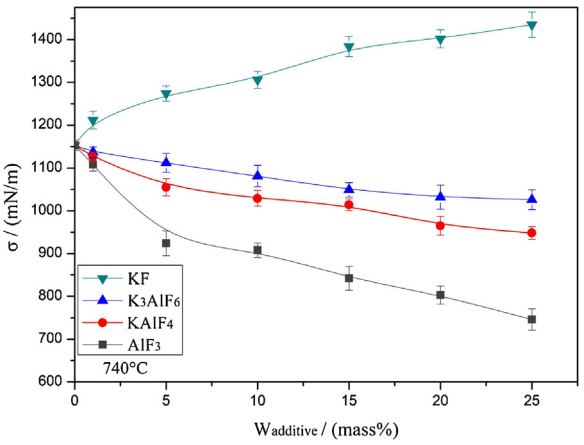


**Fig. 10 – Variation of interfacial tension between flux and alumina at 740 °C as a function of additives in equimolar NaCl-KCl salt solution.**

for pure Al melt / equimolar NaCl-KCl molten salts was measured to be 718 mN/m, and this value decreased in varying degrees as KF, $AlF_3$, $K_3AlF_6$ or $KAlF_4$ was added to the salts. For $AlF_3$ addition, the $\sigma_{F\text{-}M}$ value decreases slightly. With addition of 25 wt.% $AlF_3$, the value of $\sigma_{F\text{-}M}$ reduces to 706 mN/m. When $K_3AlF_6$ or $KAlF_4$ is added to the salts, the $\sigma_{F\text{-}M}$ value decreases continuously, and the rate of descent of the $\sigma_{F\text{-}M}$ values is more obviously compared with that in the case of $AlF_3$ addition. With additions of 25 wt.% $K_3AlF_6$ or $KAlF_4$, the value of $\sigma_{F\text{-}M}$ reduces to 625 mN/m and 640 mN/m respectively. Overall, the values of $\sigma_{F\text{-}M}$ appear to be a relative stable state with increasing $K_3AlF_6$ or $KAlF_4$ contents. Nevertheless, KF additive sharply decreases the interfacial tension, and the value of $\sigma_{F\text{-}M}$ reduces to 381 mN/m with addition of 25 wt.% KF.

Fig. 10 shows the variation of interfacial tension between flux and alumina ($\sigma_{F\text{-}I}$) at 740 °C as a function of mass% fluoride addition to equimolar NaCl-KCl. Interfacial tension for alumina / equimolar NaCl-KCl molten salts was measured to be 1153 mN/m. KF addition significantly increases the $\sigma_{F\text{-}I}$ value, while additions of $AlF_3$, $K_3AlF_6$ or $KAlF_4$ decreases the $\sigma_{F\text{-}I}$ value to various extents. With addition of 25 wt.% KF, the value of $\sigma_{F\text{-}I}$ increases to 1435 mN/m. For $K_3AlF_6$ or $KAlF_4$ additions, the $\sigma_{F\text{-}I}$ values drop slightly, and when $K_3AlF_6$ or $KAlF_4$ contents reach to 25 wt.%, corresponding $\sigma_{F\text{-}I}$ values reduce to 1026 mN/m and 948 mN/m respectively. For $AlF_3$ addition, the $\sigma_{F\text{-}I}$ values drop obviously, and with addition of 25 wt.% $AlF_3$, the value of $\sigma_{F\text{-}I}$ reduces to 746 mN/m.

It's generally believed that the decrease in interfacial tension between flux and Al melt is attributed to the adsorption of surface-active elements (such as Na or K) at the salt / aluminum interface [37–39]. In the aluminum / NaCl-KCl-KF system, as shown in Table 2, since the equilibrium constant for reaction (c) is many orders of magnitude larger than the corresponding reaction (b) in the pure NaCl-KCl system, the activity of potassium increases by several orders of magnitude with the addition of KF, causing the adsorption of K at the salt / aluminum interface increasing notably. On the other hand, in addition to the adsorption of K at the interface which promotes the observed decrease in interfacial tension, KF can react with NaCl to form NaF and KCl, and the consequent reaction (d) in Table 2 can occur, thus increasing the activity of sodium. In a word, it can be seen that the addition of KF to equimolar NaCl-KCl can increase the concentration of Na and K in the Al melt. When the amount of KF addition increases, the enrichment of Na and K at the salt / aluminum interface can take place, leading to a further remarkable decrease in interfacial tension.

In the $AlF_3$ melt, Hou et al. [40] reported that there existed few free $F^-$ ions because of the forming of Al-F-Al fluorine bridges between $Al^{3+}$ and $F^-$. Hence, in the aluminum / NaCl-KCl-$AlF_3$ system, few $F^-$ ions can be combined with $K^+$ and $Na^+$ ions to form KF and NaF, and consequently the concentrations of K and Na in the Al melt are lower due to the corresponding reaction (c) and (d) (see Table 2). Additionally, for the reverse reactions of (c) and (d), corresponding equilibrium constants are calculated to be $1.74 \times 10^8$ and $4.52 \times 10^7$ respectively. This indicates that displacement reaction between $AlF_3$ and K (or Na) can occur to a great extent. In other words, $AlF_3$ can intensely inhibit the generation of K and Na, eventually causing the difficulty of the enrichment of K and Na at the salt / aluminum interface. Therefore, when $AlF_3$ is added to equimolar NaCl-KCl, interfacial tension between flux and Al melt decreases only slightly.

In the $K_3AlF_6$ or $KAlF_4$ melt, following chemi-ionization reactions can take place [41–44]:

$$K_3AlF_6 = 3K^+ + AlF_4^- + 2F^- \quad (8)$$

$$KAlF_4 = K^+ + AlF_4^- \quad (9)$$

$$AlF_4^- = AlF_3 + F^- \quad (10)$$

With the addition of $K_3AlF_6$ (or $KAlF_4$) to equimolar NaCl-KCl, as for the aluminum / NaCl-KCl-$K_3AlF_6$ (or $KAlF_4$) system, free $F^-$ ions, originated from the above reaction (8), (9) and (10), can be combined with $K^+$ and $Na^+$ ions to form KF and NaF, and subsequently K and Na are produced by the reaction (c) and (d) (see Table 2), resulting in the observed decrease of the interfacial tension between flux and Al melt. However, note that $AlF_3$ can be produced by the reaction (10). Therefore, with the inhibiting of generation of K and Na by the $AlF_3$, the rate of descent of interfacial tension is limited to some extent. In addition, it has been revealed that the structure of $K_3AlF_6$ in liquid state is more stable than that of molten $KAlF_4$ [43–45]. Thus, the concentration of $F^-$ ions ionized from molten $K_3AlF_6$ is higher than the case of molten $KAlF_4$, ultimately causing the drop of interfacial tension for $K_3AlF_6$ addition being more evident accordingly.

As can be seen from the above results, when KF, $AlF_3$, $K_3AlF_6$ or $KAlF_4$ is added to equimolar NaCl-KCl respectively, these four fluoride salts can be classified into two categories, i.e. $AlF_3$, $K_3AlF_6$ and $KAlF_4$ being of type A and KF being of type B. The addition of A-type fluoride can decrease $\sigma_{F\text{-}M}$ slightly, and decrease $\sigma_{F\text{-}I}$ to varying degrees, while B-type additive can significantly decrease $\sigma_{F\text{-}M}$ and increase $\sigma_{F\text{-}I}$. As mentioned in section 3.1.1.4, with regard to the spreading and wetting properties of the flux, it is essential to keep the lower value of $\sigma_{F\text{-}M}$, and thus B-type additive (KF) can be considered as the fluoride component. Nevertheless, for KF addition, the lower value of

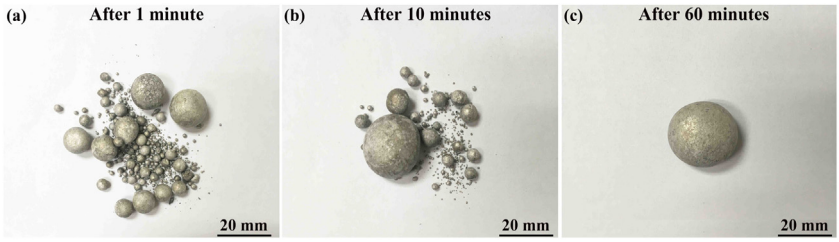


**Fig. 11 – Coalescence of aluminum droplets in NaCl-KCl-0.3 mass% KF salt solution.**

$\sigma_{F\text{-}M}$ makes it difficult for flux to be separated from Al melt, and the higher value of $\sigma_{F\text{-}I}$ is bad for the flux to wetting inclusions. Hence, in terms of single addition of KF, it is unfeasible for the flux to realize the functions of covering, drossing, and cleaning simultaneously. On the other hand, A-type additive, which can decrease $\sigma_{F\text{-}M}$ slightly, and decrease $\sigma_{F\text{-}I}$, can just offset the shortage of the single addition of KF. As a consequence, for the purpose of obtaining high-effective multifunctional characteristic for the flux, the combined addition of A-type and B-type fluoride is a better selection for fluoride component.

### 3.2.2. *Test results and discussion of oxide layer stripping ability of the flux*

As mentioned in section 3.1.2, in order to effectively evaluate oxide layer stripping ability of the flux by the tests of coalescence of aluminum droplets in salts, two interference factors, i.e. density and viscosity of molten salt, should be eliminated. Roy et al. [46] found that, when the addition of common fluoride salts (such as KF, NaF, $CaF_2$, $AlF_3$, $K_3AlF_6$, $KAlF_4$, etc.) to equimolar NaCl-KCl didn't exceed 0.5 wt.%, the density and viscosity of molten salts seemed to be almost unchanged. Hence, in the current study, 0.3 wt.% fluoride salt (KF, $AlF_3$, $K_3AlF_6$ or $KAlF_4$) was added to equimolar NaCl-KCl.

Initial morphology of aluminum chips was shown in Fig. 8(a). After the chips were immersed in the equimolar NaCl-KCl molten salt with addition of 0.3 wt.% KF, 0.3 wt.% $K_3AlF_6$, 0.3 wt.% $KAlF_4$ or 0.3 wt.% $AlF_3$, coalescence behaviors of aluminum droplets in salts as a function of time were observed, as illustrated in Fig. 11, Fig. 12, Fig. 13 and Fig. 14 respectively. As for these four different molten salts, their ability to coalesce aluminum droplets into a single melt pool could reflect directly oxide layer stripping ability of the salts. Hence, the time taken for the formation of a single drop of metal was measured for different salts. From Fig. 11, after 60 min,

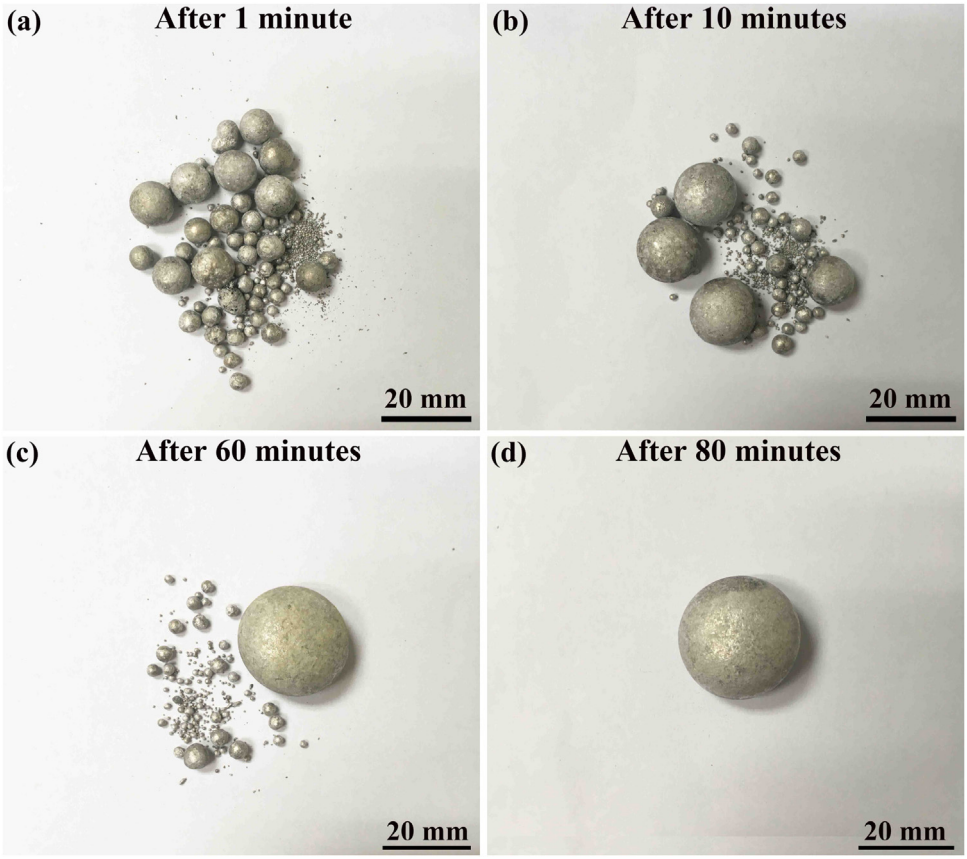


**Fig. 12 – Coalescence of aluminum droplets in NaCl-KCl-0.3 mass% $K_3AlF_6$ salt solution.**

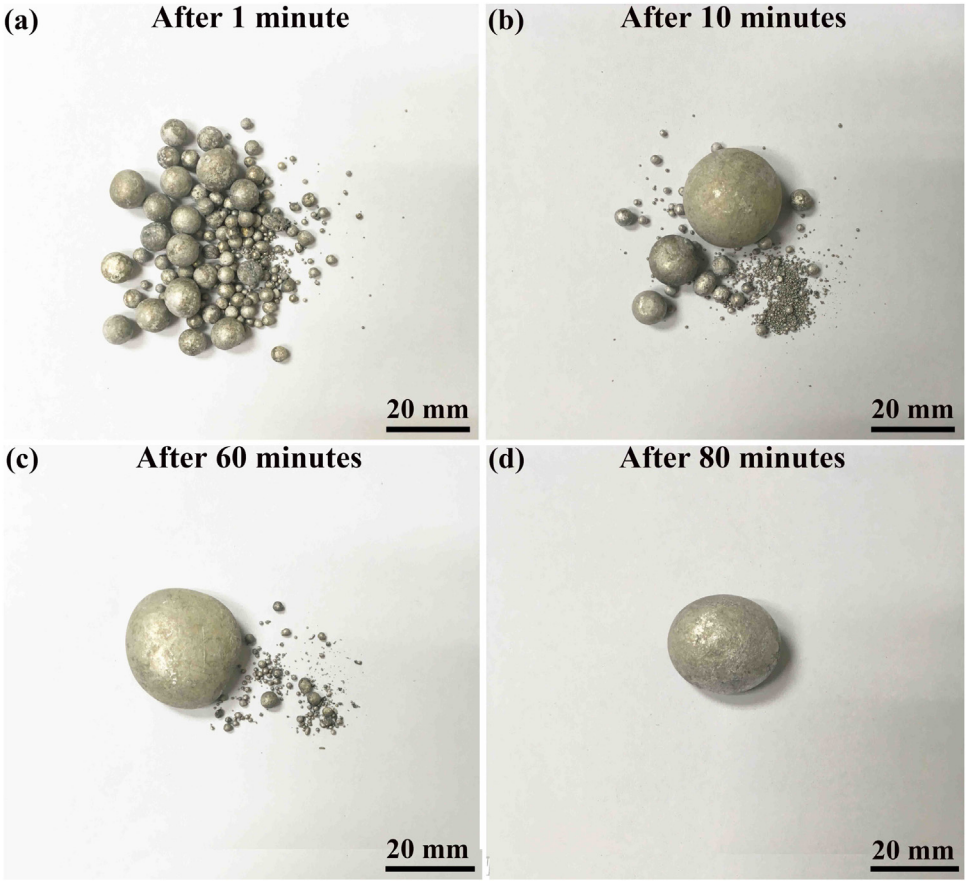


**Fig. 13 – Coalescence of aluminum droplets in NaCl-KCl-0.3 mass% $KAlF_4$ salt solution.**

a single solidified droplet could be formed due to complete coalescence for the salt containing 0.3 wt.% KF. However, in Fig. 12 and Fig. 13, after 60 min, a big metal bead and a few small metal beads were obtained, which could be attributed to the uncomplete coalescence of metal droplets in the salt containing 0.3 wt.% $K_3AlF_6$ or $KAlF_4$ at that time, and it took another 20 min for all droplets to further coalesce into one single metal droplet. Nevertheless, in Fig. 14, it can be seen that, the coalescence was not complete even after the chips were immersed in the salt containing 0.3 wt.% $AlF_3$ for 90 min, and there still existed several multi-size metal beads, which implied that the stripping of oxide layer was relatively slower. Therefore, the sequence of oxide layer stripping ability for the four fluoride salts is: KF > $K_3AlF_6$ (close to $KAlF_4$) > $AlF_3$.

When the chips were charged into the equimolar NaCl-KCl molten salt with addition of fluoride salt (such as KF, $AlF_3$, $K_3AlF_6$ or $KAlF_4$), cracks formed in the oxide layer due to chemical attack and thermal stresses, and the surface-active elements (such as Na or K) were inclined to be enriched in the cracks of oxide layer to decrease newly increased surface energy. Thus, the values of $\sigma_{F\text{-}M}$ appeared to be distributed unevenly around the molten metal surface, creating an interfacial tension gradient which consequently generated an interfacial stress [34]. Moreover, it is worth mentioning that, the more the enrichment of Na or K at the salt / aluminum interface is, the more uneven the distribution of the values of $\sigma_{F\text{-}M}$ is. This readily leads to a higher interfacial tension gradient and interfacial stress. Ultimately, it is the interfacial stress that strips the oxide layer covering the metal droplet. These conclusions are in accordance with the report by Roy and Sahai [21], who suggested that oxide layer stripping ability of salt was closely associated with the interfacial tension between salt flux and Al melt ($\sigma_{F\text{-}M}$) and the decrease of $\sigma_{F\text{-}M}$ favored the stripping of the oxide layer. As mentioned in section 3.2.1, the addition of KF to equimolar NaCl-KCl can promote abundant enrichment of Na and K at the salt / aluminum interface and sharply decrease the value of $\sigma_{F\text{-}M}$, resulting in the stronger stripping ability of oxide layer for the KF. When $AlF_3$ is added to equimolar NaCl-KCl, the enrichment of Na and K at the salt / aluminum interface is difficult and the value of $\sigma_{F\text{-}M}$ is almost unchanged, which can account for weaker stripping ability of oxide layer for the $AlF_3$. In addition, for $K_3AlF_6$ or $KAlF_4$ additions to equimolar NaCl-KCl, although the enrichment of Na and K is hindered by $AlF_3$ and the value of $\sigma_{F\text{-}M}$ decreases only slightly, the stripping of oxide layer in the molten salts is still obvious based on the observation of complete coalescence of metal droplets (see Fig. 12 and Fig. 13). This phenomenon can probably be attributed to the dissolution of oxide (often $Al_2O_3$) into molten salts containing $K_3AlF_6$ or $KAlF_4$. The reactions between $Al_2O_3$ and molten $K_3AlF_6$ or $KAlF_4$ are as follows [47–51]:

$$Al_2O_3 + AlF_6^{3-} = 3AlOF_2^- \quad (11)$$

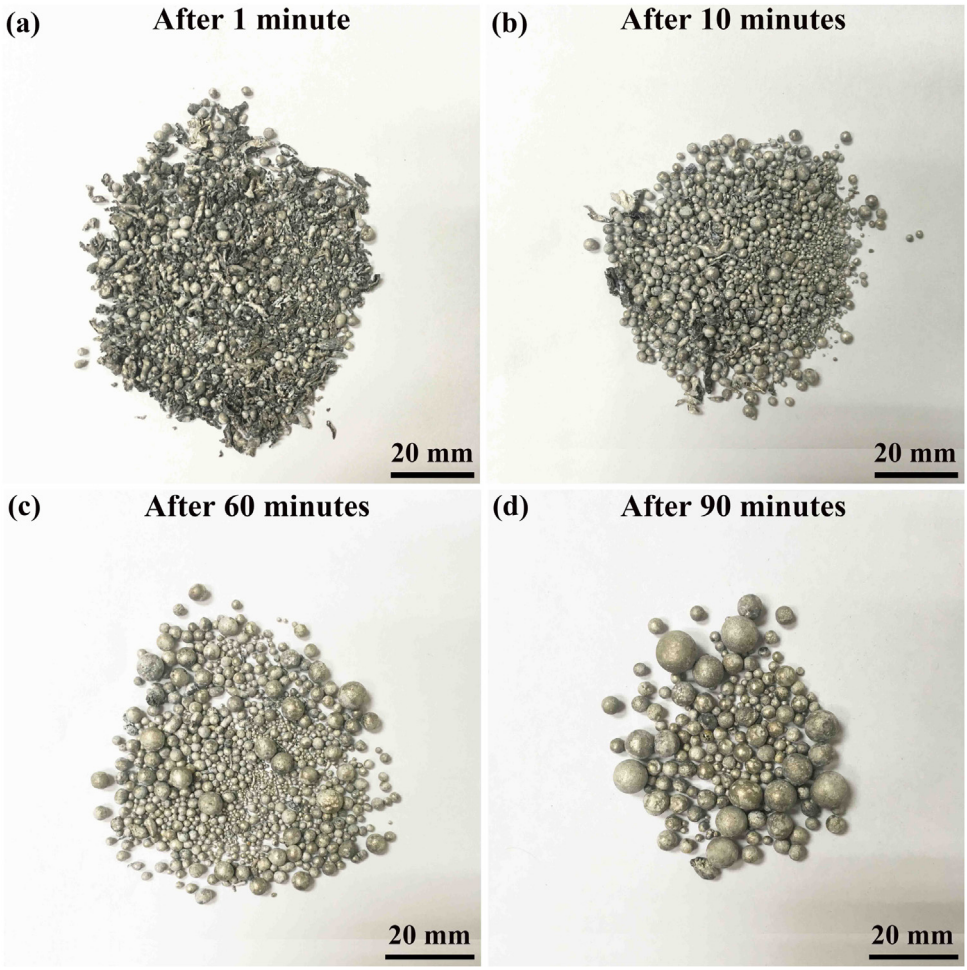


**Fig. 14 – Coalescence of aluminum droplets in NaCl-KCl-0.3 mass% $AlF_3$ salt solution.**

$$Al_2O_3+4AlF_6^{3-}=3Al_2OF_6^{2-}+6F- \quad (12)$$

$$AlF_6^{3-}=AlF_4-+2F- \quad (13)$$

$$Al_2O_3+6AlF_4^{-}=3Al_2OF_6^{2-}+2AlF_3 \quad (14)$$

$$Al_2O_3+3Al_2OF_6^{2-}=3Al_2O_2F_4^{2-}+2AlF_3 \quad (15)$$

In summary, according to the measurement results and discussion of the coalescence ability of different salts, it is clear that the stripping ability of oxide layer for KF, $K_3AlF_6$ or $KAlF_4$ is stronger while the stripping ability of oxide layer for $AlF_3$ is weaker. Additionally, considering the requirements of interfacial tensions in the Al melt-inclusion-flux system for multifunctional refining flux, the combination of KF with $K_3AlF_6$ or/and $KAlF_4$ is an optimum selection for fluoride component.

## 4. Conclusions

Based on theoretical analysis and experimental research, the optimum fluoride component in the multifunctional refining flux used for recycling aluminum scrap was determined in the present investigation. The following major conclusions can be drawn:

(1) Wettability analysis of spreading, separating, and inclusion removal properties of the flux reveals that, the lower value of $\sigma_{F\text{-}M}$ is helpful for flux to spread over the melt surface and remove solid inclusions, while excessive low value of $\sigma_{F\text{-}M}$ makes it difficult for flux to be separated from Al melt. Moreover, the lower value of $\sigma_{F\text{-}I}$ and the higher value of $\sigma_{M\text{-}I}$ are also beneficial for flux to remove solid inclusions.

(2) In terms of the Al melt, inclusion, and flux system, when KF, $AlF_3$, $K_3AlF_6$ or $KAlF_4$ was added to equimolar NaCl-KCl, it is found that, $AlF_3$, $K_3AlF_6$ or $KAlF_4$ can decrease $\sigma_{F\text{-}M}$ slightly, and decrease $\sigma_{F\text{-}I}$ to varying degrees, while KF can significantly decrease $\sigma_{F\text{-}M}$ and increase $\sigma_{F\text{-}I}$.

(3) When aluminum chips were immersed in the equimolar NaCl-KCl molten salt with addition of 0.3 wt.% KF, 0.3 wt.% $K_3AlF_6$, 0.3 wt.% $KAlF_4$ or 0.3 wt.% $AlF_3$, it is found that, the stripping ability of oxide layer for KF, $K_3AlF_6$ or $KAlF_4$ is stronger, while the stripping ability of oxide layer for $AlF_3$ is weaker. Furthermore, the stripping ability of oxide layer for $K_3AlF_6$ or $KAlF_4$ is inferior to KF.

(4) According to a comprehensive consideration of the requirements of interfacial tensions and oxide layer stripping ability for the multifunctional refining flux of recycled aluminum, the combination of KF with $K_3AlF_6$ or/and $KAlF_4$ is an optimum selection for fluoride component.

## Declaration of interests

The authors declare that they have no known competing financial interests or personal relationships that could have appeared to influence the work reported in this paper.

## Acknowledgements

The authors would like to acknowledge the financial support given by the Guangdong - Major Scientific Research Program of Higher Education of Guangdong (No. 2016KQNCX189), Special Scientific and Technological Innovation Projects of Universities of Guangdong Province (No. 2017KTSCX177), and the Opening Project of National Engineering Research Center of Near-Net-Shape Forming for Metallic Materials (South China University of Technology) (No. 2019010).

## REFERENCES

[1] Krishnan PK, Christy JV, Arunachalam R, Mourad AHI, Muraliraja R, Al-Maharbi M, et al. Production of aluminum alloy-based metal matrix composites using scrap aluminum alloy and waste materials: influence on microstructure and mechanical properties. J Alloys Compd 2019;784:1047–61.
[2] Martin JH, Yahata BD, Hundley JM, Mayer JA, Schaedler TA, Pollock TM. 3D printing of high-strength aluminium alloys. Nature 2017;549:365–9.
[3] Yang T, Wang KS, Wang W, Peng P, Huang LY, Qiao K, et al. Effect of friction stir processing on microstructure and mechanical properties of AlSi10Mg aluminum alloy produced by selective laser melting. JOM 2019;71:1737–47.
[4] Fox S, Campbell J. Visualisation of oxide film defects during solidification of aluminium alloys. Scripta Mater 2000;43:881–6.
[5] Schlesinger ME. Aluminum recycling. Boca Raton: CRC Press; 2007.
[6] Zhou M, Li K, Sun BD, Shu D, Ni HJ, Wang J. A fluxing method to remove inclusions from molten aluminum. J Mater Sci Lett 2002;21:1285–7.
[7] Cao X, Campbell J. Oxide inclusion defects in Al-Si-Mg cast alloys. Can Metall Quart 2005;44:435–48.
[8] Liu SG, Cao FY, Zhao XY, Jia YD, Ning ZL, Sun JF. Characteristics of mold filling and entrainment of oxide film in low pressure casting of A356 alloy. Mater Sci Eng A 2015;626:159–64.
[9] Raiszadeh R, Griffiths WD. The behaviour of double oxide film defects in liquid Al alloys under atmospheric and reduced pressures. J Alloys Compd 2010;491:575–80.
[10] Damoah LNW, Zhang LF. Removal of inclusions from aluminum through filtration. Metall Mater Trans B 2010;41B:886–907.
[11] Majidi O, Shabestari SG, Aboutalebi MR. Study of fluxing temperature in molten aluminum refining process. J Mater Process Tech 2007;182:450–5.
[12] Espinoza-Cuadra J, García-García G, Mancha-Molinar H. Influence of defects on strength of industrial aluminum alloy Al–Si 319. Mater Design 2007;28:1038–44.
[13] Ni HJ, Sun BD, Jiang HY, Ding WJ. Effects of rotating impeller degassing on microstructure and mechanical properties of the A356 scraps. Mater Sci Eng A 2003;352:294–9.
[14] Li C, Li JG, Mao YZ, Ji JC. Mechanism to remove oxide inclusions from molten aluminum by solid fluxes refining method. China Foundry 2017;14:233–43.
[15] Utigard TA, Friesen K, Roy RR, Lim J, Silny A, Dupuis C. The properties and uses of fluxes in molten aluminum processing. JOM 1998;50:38–43.
[16] Utigard TA, Roy RR, Friesen K. The roles of molten salts in the treatment of aluminum. Can Metall Quart 2001;40:327–34.
[17] Chen YJ. Ultrasonic evaluation of the quality of A356.2 alloy by fluxing treatment. Mater Trans 2010;51:803–9.
[18] Hiraki T, Miki T, Nakajima K, Matsubae K, Nakamura S, Nagasaka T. Thermodynamic analysis for the refining ability of salt flux for aluminum recycling. Materials 2014;7:5543–53.
[19] Tenorio JAS, Carboni MC, Espinosa DCR. Recycling of aluminum-effect of fluoride additions on the salt viscosity and on the alumina dissolution. J Light Met 2001;1:195–8.
[20] Ye J, Sahai Y. Role of molten salt flux in melting of used beverage container (UBC) scrap. In: In: proceedings of the third international symposium recycling of metals and engineered materials. Warrendale: TMS; 1995. p. 639–50.
[21] Roy RR, Sahai Y. Coalescence behavior of aluminum alloy drops in molten salts. Mater Trans JIM 1997;38:995–1003.
[22] Besson S, Pichat A, Xolin E, Chartrand P, Friedrich B. Improving coalescence in Al-Recycling by salt optimization. in: proceedings of EMC; 2011. p. 1–16.
[23] Xiao Y, Reuter MA, Boin U. Aluminium recycling and environmental issues of salt slag treatment. J Environ Sci Heal A 2005;40:1861–75.
[24] Xiao Y, Reuter MA. Recycling of distributed aluminium turning scrap. Miner Eng 2002;15:963–70.
[25] Damoah LNW, Zhang LF. $AlF_3$ reactive $Al_2O_3$ foam filter for the removal of dissolved impurities from molten aluminum: preliminary results. Acta Mater 2011;59, 896–13.
[26] Ware TN, Dahle AK, Charles S, Couper MJ. Effect of Sr, Na, Ca & P on the castability of foundry alloy A356.2. 2nd international aluminium casting technology symposium; 2002. Ohio, USA.
[27] Tiedje NS, Taylor JA, Easton MA. Feeding and distribution of porosity in cast Al-Si alloys as function of alloy composition and modification. Metall Mater Trans A 2012;43:4846–58.
[28] Bashforth F, Adams JC. An attempt to test the theories of capillary action. London: Cambridge University Press; 1883.
[29] Roy RR, Sahai Y. Wetting behavior in aluminum-alumina-Salt systems. Mater Trans JIM 1997;38:571–4.
[30] Grjotheim K, Krohn C, Malinovsky M, Matiasovsky K, Thonstad J. Aluminium electrolysis: fundamentals of the hall-heroult process. 2nd ed. Dusseldorf: Aluminium-Verlag; 1982.
[31] Myers D. Surfaces, interfaces, and colloids: principles and applications. second edition New York: John Wiley & Sons, Inc.; 1999.
[32] Eustathopoulos N, Nicholas MG, Drevet B. Wettability at high temperatures. UK: Elsevier Science Ltd; 1999.
[33] Zhu GL, Xiao YP, Yang YX, Wang J, Sun BD, Boom R. Recycling of aluminum from fibre metal laminates. J Shanghai Jiaotong Univ (Sci) 2012;17:263–7.
[34] Ye J, Sahai Y. Interfacial behavior and coalescence of aluminum drops in molten salts. Mater Trans JIM 1996;37:175–80.
[35] Muric-Nesic J, Compston P, Noble N, Stachurski ZH. Effect of low frequency vibrations on void content in composite materials. Compos Part A Appl Sci Manuf 2009;40:548–51.

[36] Tenorio JAS, Espinosa DCR. Effect of salt/oxide interaction on the process of aluminum recycling. J Light Met 2002;2:89–93.
[37] Silny A, Utigard TA. Interfacial tension between aluminum and chloride–Fluoride melts. J Chem Eng Data 1996;41:1340–5.
[38] Roy RR, Sahai Y. Interfacial tension between aluminum alloy and molten salt flux. Mater Trans JIM 1997;38:546–52.
[39] Roy RR, Utigard TA. Interfacial tension between aluminum and NaCl-KCl-based salt systems. Metall Mater Trans B 1998;29B:821–7.
[40] Hou HY, Xie G, Chen SR, Zhang XF. Structure of molecular dynamics simulated NaF-$AlF_3$ melt. Chin J Nonferrous Met 2000;10:914–8 (In Chinese).
[41] Robert E, Lacassagne V, Bessada C, Massiot D, Gilbert B, Coutures JP. Study of NaF-$AlF_3$ melts by high-temperature $^{27}Al$ NMR spectroscopy: comparison with results from Raman spectroscopy. Inorg Chem 1999;38:214–7.
[42] Foster PA. Phase equilibria in the system $Na_3AlF_6$-$AlF_3$. J Am Ceram Soc 1970;53:598–600.
[43] Bruno M, Herstad O, Holm JL. Stability and structure of sodium tetrafluoroaluminate, $NaAlF_4$. Acta Chem Scand 1998;52:1399–401.
[44] Phillips B, Warshaw CM, Mockrin I. Equilibria in $KAlF_4$ containing systems. J Am Ceram Soc 1966;49:631–4.
[45] Thompson WT, Goad DGW. Some thermodynamics properties of $K_3AlF_6$-$KAlF_4$ melts. Can J Chem 1976;54:3342–9.
[46] Roy RR Ye J, Sahai Y. Viscosity and density of molten salts based on equimolar NaCl-KCl. Mater Trans JIM 1997;38:566–70.
[47] Zhou M, Shu D, Li K, Zhang WY, Sun BD, Wang J, et al. Performance improvement of industrial pure aluminum treated by stirring molten fluxes. Mater Sci Eng A 2003;347:280–90.
[48] Zhang YS, Wu XX, Rapp RA. Solubility of alumina in cryolite melts: measurements and modeling at 1300 K. Metall Mater Trans B 2003;34B:235–42.
[49] Zhang YS, Rapp RA. Modeling the dependence of alumina solubility on temperature and melt composition in cryolite-based melts. Metall Mater Trans B 2004;35B:509–15.
[50] Rakhmatullin A, Keppert M, Šimko F, Bessada C. Aluminium phosphate behaviour in $Na_3AlF_6$-$Al_2O_3$ melts: a new insight from in situ high temperature NMR measurements. New J Chem 2016;40:1737–41.
[51] Lacassagne V, Bessada C, Florian P, Bouvet S, Ollivier B, Coutures JP, et al. Structure of high-temperature NaF-$AlF_3$-$Al_2O_3$ melts: a multinuclear NMR study. J Phys Chem B 2002;106:1862–8.